

Cite this: DOI: 10.1039/c8dt00619a

Stable ruthenium olefin metathesis catalysts bearing symmetrical NHC ligands with primary and secondary *N*-alkyl groups†

Chiara Ambrosio,^a Veronica Paradiso,^a Chiara Costabile,^a Valerio Bertolasi,^b Tonino Caruso^a and Fabia Grisi^{a*}

Four novel stable Hoveyda–Grubbs-type catalysts containing *N,N'*-dineopentyl- and *N,N'*-dicyclohexyl-substituted *N*-heterocyclic carbene (NHC) ligands with *syn* and *anti* phenyl groups on the ring backbone were synthesized and fully characterized. The catalytic potential of these complexes was investigated in metathesis reactions of both standard and renewable substrates. Compared to the Hoveyda–Grubbs second generation catalyst (**HGII**), all of the new catalysts showed high performances in most of the examined metathesis transformations. In particular, *N,N'*-dicyclohexyl catalysts gave improved results in the challenging ring-closing metathesis (RCM) reaction to form tetrasubstituted olefins, while catalysts with neopentyl *N*-groups were found to be more active and *Z*-selective in cross-metathesis (CM) reactions. Modest enantioselectivities in the asymmetric ring-closing metathesis (ARCM) of achiral trienes with different steric hindrance were observed in the presence of catalysts bearing chiral *C*₂-symmetric NHC ligands.

Received 14th February 2018,

Accepted 11th April 2018

DOI: 10.1039/c8dt00619a

rsc.li/dalton

Introduction

Since their introduction more than 25 years ago,¹ *N*-heterocyclic carbenes (NHCs) have emerged as an important class of ligands in transition metal mediated processes and have also been used as valuable nucleophilic organocatalysts in a series of organic reactions.² The tremendous success of NHCs reflects their unique stereoelectronic properties and finds maximum expression in their application as ancillary ligands for ruthenium-based olefin metathesis catalysts.³ Indeed, due to the easy manipulation of the NHC scaffold of classical second generation catalysts (*e.g.* **GII** and **HGII**, Chart 1), many NHC ligands have been designed to confer specific catalytic properties to the resulting ruthenium-based catalysts in metathesis applications.⁴

In this context, a fair number of modifications of the NHC ligand have been gained by varying the steric and electronic properties of substituents on the backbone and/or the nitrogen atoms, leading to the development of systems with improved stability, activity and selectivity.⁵ While ruthenium olefin metathesis complexes bearing saturated NHC ligands with aryl side

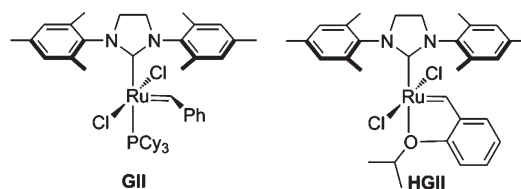


Chart 1 Grubbs and Hoveyda–Grubbs second generation catalysts.

chains have been thoroughly investigated,^{4,5} only a very few number of analogous ruthenium complexes with aliphatic amino side groups have been documented until now (see 1–3, Chart 2).⁶ What is more, all of them present secondary *N*-alkyl groups. The synthetic access to ruthenium complexes containing saturated NHCs with *N*-alkyl groups has been strongly limited by the tendency of NHCs with small *N*-alkyl groups to dimerize rather than to form the corresponding metal complex^{7a} and by the inability of NHCs presenting extremely bulky aliphatic amino groups to be accommodated in the coordination sphere of the metal complex.⁷ In addition, some of these complexes, albeit observed, were not stable enough to be isolated.^{6a} For all these reasons, an in-depth study of the catalytic properties of this class of complexes and a full evaluation of the influence exerted by the *N*-alkyl substituents on the efficiency of catalysts have not been available to date.

With this in mind, we aimed to develop stable *N,N'*-dialkyl substituted ruthenium complexes by modifying the steric properties and flexibility of the NHC ring due to the presence of

^aDipartimento di Chimica e Biologia “Adolfo Zambelli”, Università di Salerno, Via Giovanni Paolo II 132, I-84084 Fisciano, Salerno, Italy. E-mail: fgrisi@unisa.it

^bDipartimento di Chimica and Centro di Strutturistica Diffraattometrica, Università di Ferrara, Via L. Borsari 46, I-44100 Ferrara, Italy

† Electronic supplementary information (ESI) available. CCDC 1564122. For ESI and crystallographic data in CIF or other electronic format see DOI: 10.1039/c8dt00619a

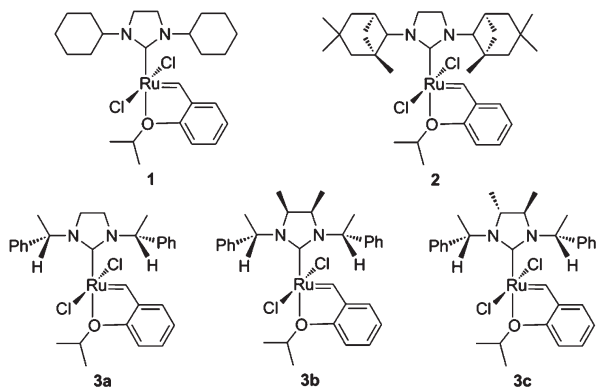


Chart 2 Ruthenium catalysts with aliphatic amino side groups.

suitable substituents on the NHC backbone. We hypothesized that, through this modification, the tendency of NHCs to dimerize could be limited, allowing for the formation of the desired metal complexes more easily. Furthermore, we reasonably expected that backbone substitution would have a positive impact on the stability of complexes, as already observed for both N,N' -diaryl^{5e,f,8} and N -alkyl/ N' -aryl⁹ catalysts, and that installation on the NHC backbone of groups with a precise stereochemical relationship (*syn* or *anti*) could alter the properties of the resulting catalysts.¹⁰ Thus, in the present work we report on the synthesis and characterization of four new Hoveyda–Grubbs second generation type complexes decorated with NHC ligands which combine different alkyl groups on the nitrogen atoms (neopentyl or cyclohexyl) and *syn*- or *anti*-related phenyl groups on the backbone (4–7, Chart 3). Notably, metathesis ruthenium complexes bearing saturated NHC ligands containing primary N -alkyl groups (4 and 5) are described for the first time. Indeed, to the best of our knowledge, the only known examples of NHC–olefin metathesis cata-

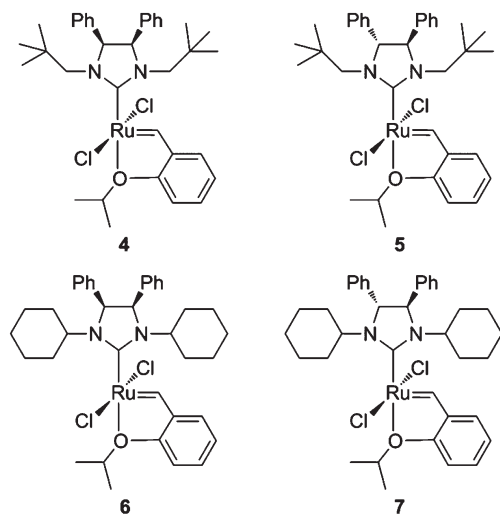


Chart 3 New ruthenium complexes with N,N' -dialkyl substituted NHC ligands.

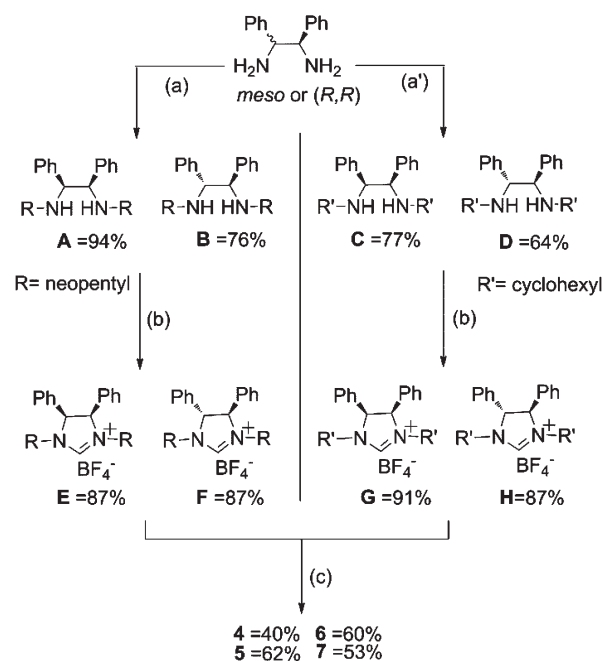
lysts containing primary N -alkyl groups are bis(NHC) complexes where the alkyl-substituted NHC is unsaturated.¹¹

The steric and electronic features of newly developed complexes 4–7 were assessed through both experimental and theoretical studies, and their catalytic performances were evaluated in typical ring-closing metathesis (RCM), cross-metathesis (CM) and ring-opening metathesis polymerization (ROMP) reactions as well as in RCM and CM metathesis transformations involving renewable compounds. Finally, the catalytic potential of 5 and 7, possessing chiral C_2 -symmetric NHC ligands, was also evaluated in the enantioselective desymmetrization of achiral trienes *via* asymmetric ring-closing metathesis (ARCM).

Results and discussion

Synthesis and characterization of complexes 4–7

The synthesis of complexes 4–7 was easily accomplished starting from commercial *meso*- or (R,R)-1,2-diphenylethylenediamine, as depicted in Scheme 1. The dialkylated diamines **A**, **B**, and **C** were obtained by a condensation reaction



Scheme 1 Synthesis of ruthenium complexes 4–7. Reaction conditions: (a) (1) *meso*-1,2-Diphenylethylenediamine (for **A**) or (R,R)-diphenylethylenediamine (for **B**), pivalaldehyde, CH_2Cl_2 , molecular sieves, room temperature, 48 h; (2) NaBH_4 , CH_3OH , room temperature, 3.5 h. (a') For **C**: (1) *meso*-1,2-diphenylethylenediamine, cyclohexanone, CH_2Cl_2 , molecular sieves, room temperature, 48 h; (2) NaBH_4 , CH_3OH , room temperature, 3.5 h. For **D**: (1) (R,R)-diphenylethylenediamine, cyclohexanone, CH_2Cl_2 , molecular sieves, room temperature, 12 h; (2) NaBH_4 , CH_3OH , room temperature, 3.5 h; (3) cyclohexanone, HCOOH , CHCl_3 , molecular sieves, 50 °C, 48 h; (4) NaBH_4 , CH_3OH , room temperature, 3.5 h. (b) NH_4BF_4 , $\text{CH}(\text{OEt})_3$, 135 °C, 2 h. (c) $(\text{CF}_3)_2\text{CH}_3\text{COK}$, **HGI**, toluene, 65 °C, 50 min (for **4**, **6** and **7**).

with pivalaldehyde (**A**, **B**) or cyclohexanone (**C**) followed by reduction *in situ* of the resulting diimines with sodium borohydride (76–94% yields), whereas diamine **D** was prepared by two subsequent steps of reductive amination with cyclohexanone (64% yield), since following the same synthetic route used for **A–C** lower yields of **D** (~20%) were registered. The NHC precursors **E–H** were all obtained in high yields (87–91%) after reaction of the respective diamines with triethyl orthoformate and ammonium tetrafluoroborate. The treatment of **E–H** with the appropriate base (potassium hexafluoro-*t*-butoxide or potassium *t*-amylate) in the presence of $\text{RuCl}_2(\text{=CH-}o\text{-iPrO-Ph})(\text{PCy}_3)$ (**HGI**) led to the desired complexes **4–7** as air- and moisture-stable green solids (40–62% yields).¹²

All the complexes were characterized by NMR spectroscopy, elemental analysis and ESI-FT-ICR analysis. Single crystals of

complex **6** were grown by the slow diffusion of pentane into a concentrated solution of diethyl ether. The solid state structure of **6** was obtained by X-ray diffraction studies and is shown in Fig. 1. In this compound, the Ru center is penta-coordinated and adopts a distorted square pyramidal coordination geometry. The Cl atoms are *trans* oriented in the basal plane and the carbene C1 atom is in the *trans* position with respect to the O1 oxygen of the 2-*i*PrO substituent at the benzylidene ligand, which is rotated by 22.23(4)° with respect to the NHC ring. Compound **6** crystallizes in the centro-symmetric $P2_1/c$ space group with the NHC phenyl groups in the *cis* position with respect to the C2–C3 bond. Accordingly, the crystal contains a racemic mixture of both the enantiomers having opposite configurations (*SR* or *RS*) at the C2 and C3 asymmetric carbon atoms. The rotations of the cyclohexane rings at the N1 and N2 NHC atoms are mainly determined by short intramolecular interactions: $\text{H20}\cdots\text{Ru1} = 2.9206(3)$ Å and $\text{H14}\cdots\text{Cl2} = 2.805(1)$ Å.

Despite numerous attempts, we were not able to grow crystals of **4**, **5** and **7** suitable for X-ray analysis due to their high solubility in most common solvents.

To support characterization of **4–7**, minimum energy structures were located for all complexes by density functional theory (DFT) studies and are shown in Fig. 2 (see the ESI† for further details).

Top and side views of minimum energy structures of **4–7**, displayed in Fig. 2, show how the orientation of *N*-substituents is influenced by the phenyls on the backbone. It is worth noting also that the torsion angles of the NHC planes with respect to the alkylidene group are very pronounced for **6** and **7** (28.5° and –31.8°, respectively) due to the steric interactions between the cyclohexyl and alkylidene groups.

Thermal stabilities of **4–7** were evaluated in C_6D_6 solutions at 60 °C under nitrogen and monitored by ^1H NMR spectroscopy over 40 days using tetrakis(trimethylsilyl)silane as an internal standard. The degradation process of each complex (20 days) is illustrated in Fig. 3.

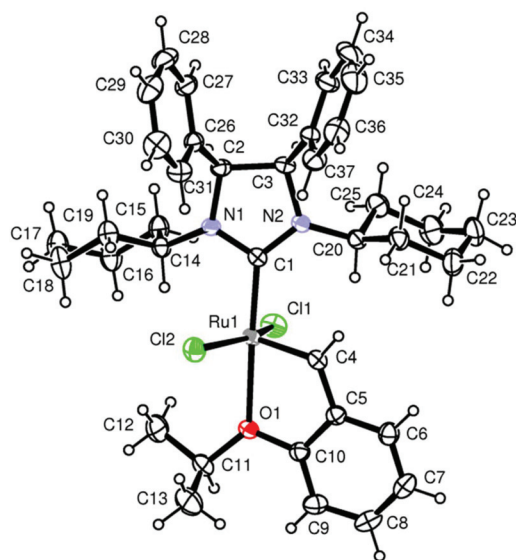


Fig. 1 ORTEP¹³ view of **6** showing the thermal ellipsoids at the 40% probability level.

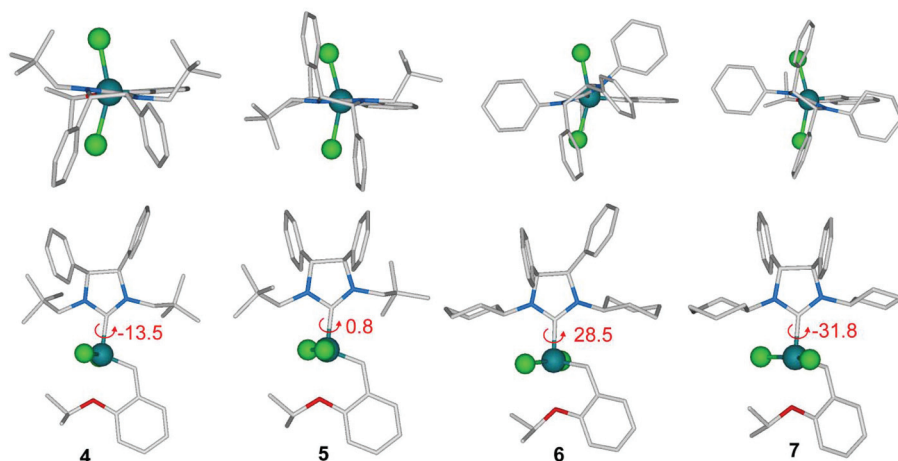


Fig. 2 Top and side views of the calculated minimum energy structures of **4–7**.

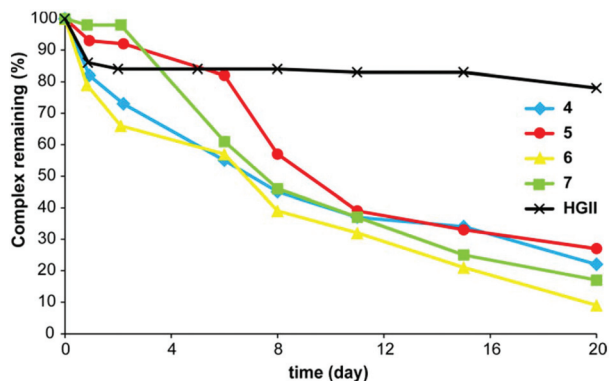


Fig. 3 Stability tests of 4–7 in C_6D_6 at 60 °C under nitrogen. Decomposition was monitored by 1H NMR spectroscopy using tetrakis(trimethylsilyl)silane as an internal standard. The lines are intended as a visual aid only.

Complexes 4 and 5 with neopentyl *N*-substituents were found to be more stable compared to 6 and 7 having cyclohexyl *N*-substituents. Moreover, although after 20 days the amount of the residual complex was quite similar for both the couples of *syn* and *anti* diastereomers, *anti* complexes showed higher stability than the corresponding *syn* isomers, mainly in the first 5–8 days of analysis. After 40 days, only 5 still persisted (14% of unaltered complex). On the whole, 4–7 displayed good stabilities when compared to unsymmetrical systems bearing an analogous *N*-alkyl moiety,^{9c} albeit they were all definitely less robust than the classical **HGII** complex with *N*-aromatic substituents over a long period of time.

To provide a more complete characterization of the newly developed complexes 4–7, the steric and electronic properties of the corresponding NHC ligands were investigated. Since crystal data were available only for complex 6, steric para-

eters were assessed by calculating percent buried volumes ($\%V_{Bur}$) and producing steric maps (Fig. 4) from the density functional theory (DFT) optimized geometries of 4–7 (see Fig. 2)¹⁴ (see the ESI† for computational details).

No remarkable differences could be appreciated between the overall NHC $\%V_{Bur}$ of *syn* and *anti* isomers with the same *N*-substituents, whereas complexes having *N*-neopentyl substituents present an overall $\%V_{Bur}$ higher than those with *N*-cyclohexyl ones (see also Table 1). Moreover, complexes with *N*-neopentyl substituents (4–5) show an asymmetrical hindrance located in a specific quadrant, which means that the NHC ligand crowds the reacting side of the metal deeply just in a small area (orange area of the map), whereas the steric encumbrance is more diffuse as for complexes with *N*-cyclohexyl substituents (6–7). Compared to **HGII** (Fig. 5), 4–7 have lower overall NHC $\%V_{Bur}$ values and a less symmetrically distributed steric pressure around the metal.

As already reported in the literature,^{9c,15} differences in stability displayed by complexes 4–7 can be mainly related to small differences in the steric demands of the corresponding NHCs. In this view, complexes with bulkier ligands are more stable than those with less encumbered ligands: **HGII** > 5 \approx 4 > 7 \approx 6.

To depict a complete description of 4–7, the electronic properties of the corresponding NHCs were assessed by experimental and theoretical investigations. More in detail, electrochemical studies were performed to evaluate the electron-donating abilities of the NHC ligands of 4–7.¹⁶ The Ru(II)/Ru(III) redox potentials determined by cyclic voltammetry are shown in Table 1.

A slight influence of the *N*-alkyl substitution within the NHC framework on the electron density at the ruthenium center was proved by differences in redox potentials (24–50 mV) between complexes 4–5 and 6–7. In particular, the

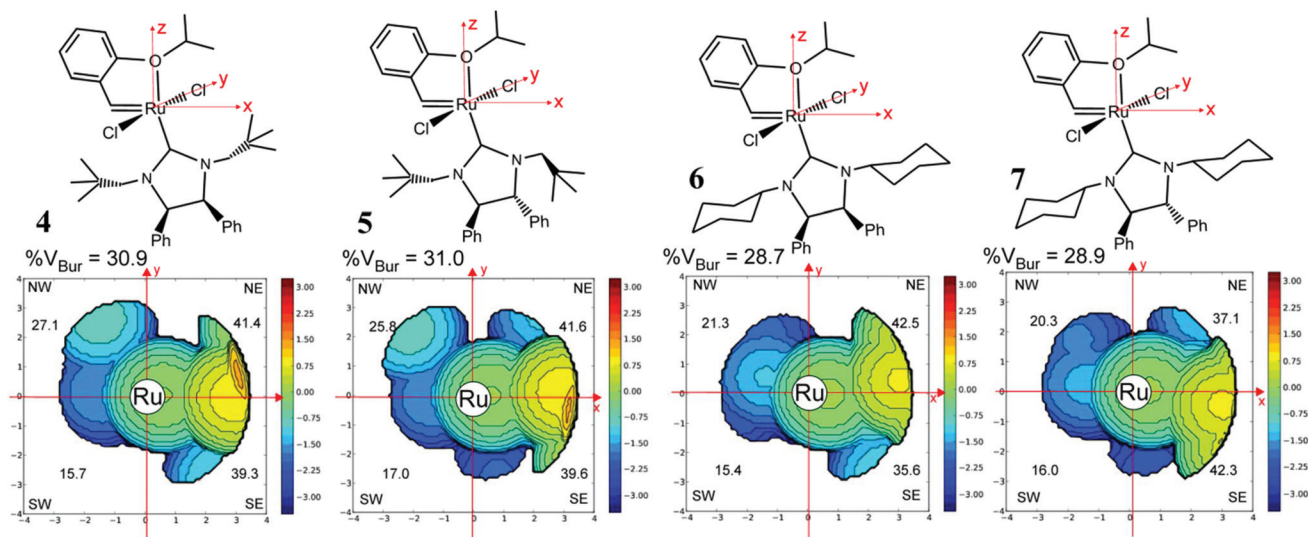


Fig. 4 Topographic steric maps of 4–7. The iso-contour curves of steric maps are in Å. The maps were constructed starting from the minimum energy structures of complexes optimized by DFT calculations. The complexes are oriented according to the complex scheme. Overall $\%V_{Bur}$ and $\%V_{Bur}$ representative of each single quadrant are reported for each map.

Table 1 Percent buried volumes, redox potentials and bond-dissociation energies for 4–7

Complex	%V _{Bur} ^a	$\Delta E_{1/2}$ ^b (V)	BDE ^c (kcal mol ⁻¹)
4	30.9	0.996	-64.9
5	31.0	1.00	-66.0
6	28.7	0.972	-73.5
7	28.9	0.950	-71.5
HGII	32.9	0.860 ^d	-70.9

^a Percent buried volume obtained from DFT optimized structures.

^b Redox potentials determined using cyclic voltammetry in CH₂Cl₂ under nitrogen; 1 mM analyte, 0.1 M NBu₄PF₆ as supporting electrolyte and 1 mM octamethylferrocene as an internal standard. Scan rate: 100 mV s⁻¹. ^c Bond-dissociation energies are referred to the Ru–NHC bond. ^d Redox potential reported in the literature¹⁶ is 0.850 V.

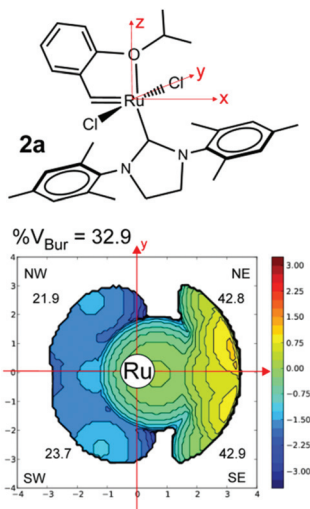


Fig. 5 Topographic steric map of **HGII**. The iso-contour curves of steric maps are in Å. The map was constructed starting from the minimum energy structures of complex optimized by DFT calculations. The complex is oriented according to the complex scheme. Overall %V_{Bur} and %V_{Bur} representative of each single quadrant are reported in the map.

presence of *N*-cyclohexyl substituents (6–7) confers better electron donating properties to the corresponding NHCs. Moreover, in the case of *N*-cyclohexyl complexes a small effect of the NHC backbone configuration on the electron donor properties was observed, as revealed by a cathodic shift of 22 mV registered moving from the *syn* isomer **6** to *anti* **7**. This shift implies an increased electron density at the metal center. Compared to commercial *N,N'*-diaryl substituted **HGII**, all the complexes displayed anodic shifts of the Ru(II)/Ru(III) redox potentials (90–150 mV), suggesting lower electron donating abilities of the related NHCs. Since similar values of redox potentials were observed for both ruthenium complexes bearing symmetrical and unsymmetrical NHCs with phenyl groups on the backbone, it is reasonable to ascribe the lower donor ability mainly to the backbone substitution rather than to the presence of *N,N*-dialkyl substituents.^{5j,9c} The σ -donor character of the NHCs of 4–7 was also estimated on the basis

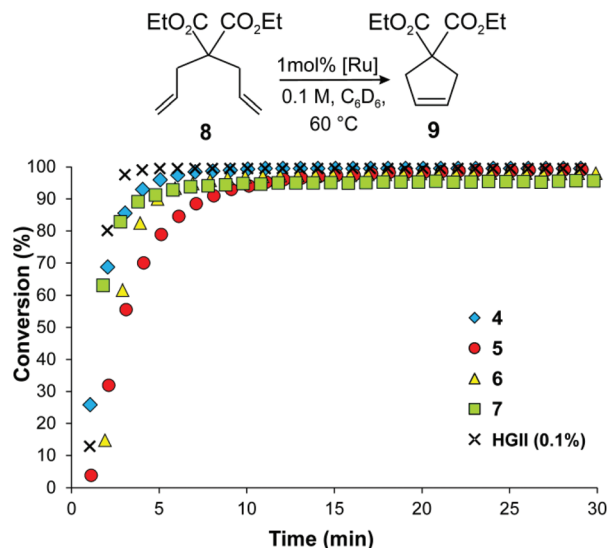
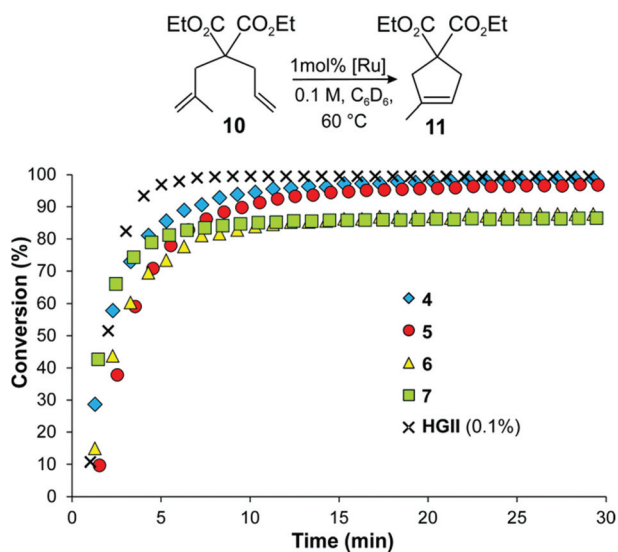
of a recent method that makes use of ¹³C NMR spectroscopy.¹⁷ It has been shown that the ¹J_{CH} coupling constant between the carbon and the hydrogen atom of the precarbenic position in the azolium salts can be used to evaluate the σ -electron donor of the respective NHCs. The higher the ¹J_{CH}, the poorer the σ -donation ability.¹⁸ The ¹J_{CH} values of 205 and 206 Hz were measured for **E** and **F**, respectively, indicating that in this case a different NHC backbone configuration has basically no effect on the σ -donor properties of the carbene. On the other hand, for **G** (¹J_{CH} = 201 Hz) and **H** (¹J_{CH} = 204 Hz) the presence of the *syn* oriented phenyl groups on the backbone appears to enhance the σ -donor ability of the corresponding NHC. By comparison of these values with that reported for the NHC precursor of the **HGII** (¹J_{CH} = 206 Hz),^{17a} it appears that the NHCs derived from salts **E**, **F** and **H** present quite similar σ -donor properties, while the NHC generated from **G** is a slightly better σ -donor. It must be noted, however, that the overall electron density of the metal depends on the σ -donation, as well as on the π -donation to the metal and on the π -back donation from the metal to the NHC ligand;¹⁹ therefore some inconsistencies in information deriving from ¹J_{CH} and redox potential measurements are expectable.

Bond-dissociation energies (BDEs) of the Ru–NHC bonds in complexes 4–7 were also evaluated by DFT calculations and are shown in Table 1. While, once again, no correlation was found among BDE values and electronic parameters (as $\Delta E_{1/2}$), BDEs appear meaningful when compared with %V_{Bur}. In fact, less hindered ligands, such as *N*-cyclohexyl substituted NHC, show higher BDE values with respect to the more crowded neopentyl *N*-substituted NHCs. Comparison with *N*-mesityl NHC is not significant since *N*-substituents with sp² *N*-carbons create a different encumbrance around the metal.

Catalytic behaviours of 4–7

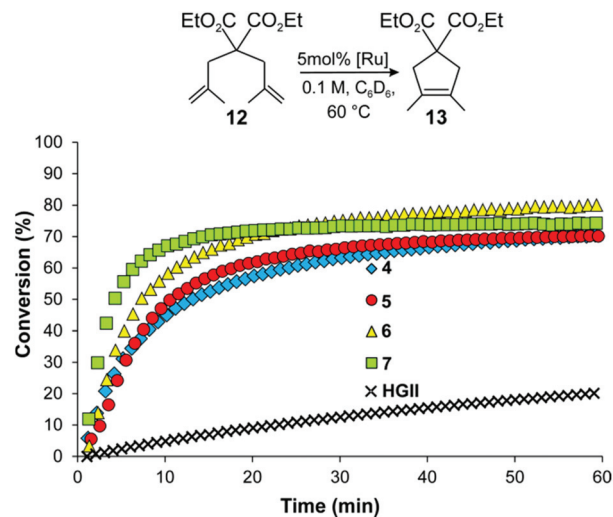
The catalytic performances of new complexes 4–7 were first investigated in model RCM reactions of malonate derivatives with increasing steric demand (**8**, **10**, and **12**). All the ring-closures were monitored over time by ¹H NMR spectroscopy and the corresponding kinetic profiles are sketched in Fig. 6–8. To put the results into a larger context, conversion–time curves for parallel RCM reactions carried out with the commercial catalyst **HGII** are also displayed.

In the RCM of **8** (Fig. 6), 4–7 showed similar catalytic activities, with catalyst **4** performing slightly better than all the other ones (>98% conversion in 10 min) and disclosing a higher reaction rate compared to its *anti* isomer **5**. All the four complexes were found to be less efficient than commercial **HGII** at a tenfold lower catalyst loading. Reactivity differences among the newly developed catalysts can be better appreciated in the RCM of the more encumbered diethyl allylmethylmalonate (**10**). As shown by the kinetic plots in Fig. 7, **4** and **5** were able to nearly complete the cyclization reaction (>97% conversion) within 30 min, outperforming **6** and **7** which reached plateau conversion values of 88 and 86%, respectively, after roughly 10 min. Moreover, while it seems that the nature of the *N*-alkyl substituents has a role in modulating catalytic

Fig. 6 RCM conversion of **8**.Fig. 7 RCM conversion of **10**.

behavior, the different NHC backbone configurations (*syn* or *anti*) seem to somewhat have an influence only on the initiation rates of the catalysts. Again, lower catalyst efficiency with respect to **HGII** was registered.

In the most sterically demanding RCM of diethyl dimethylmalonate (**12**) (Fig. 8), differently from the previous cyclization reaction, the catalytic performances of catalysts **6** and **7** were superior to those of **4** and **5**, displaying faster initiation and faster reaction rates. The maximum value conversion (80%) was observed in the presence of **6**; in fact catalyst **7**, despite the higher initiation rate, showed a significant decrease in the reaction rate after the first 10 min, reaching a plateau at 74% conversion. Interestingly, all the new catalysts were found to be more efficient than commercially available **HGII** which

Fig. 8 RCM conversion of **12**.

gave only 20% conversion within 60 min. Moreover, they proved to have activities superior to most of the catalysts supported by symmetrical *N,N'*-diaryl substituted NHCs.²⁰

The above results seem to suggest that the RCM catalytic behavior shown by these catalysts is essentially controlled by steric factors. Indeed, as already reported in the literature, most of the catalysts with encumbered NHC ligands^{21,5j,8b} speed up the RCM of unhindered olefins (such as diethyl diallylmalonate and diethyl allylmethylmalonate) and slow down the RCM of hindered olefins (such as diethyl dimethylmalonate). Comparison among catalysts **4**–**7** seems to show the same trend. Complexes **4**–**5**, which appear to be more hindered from topographic maps and %*V*_{Bur} values (%*V*_{Bur} = 30.9 and 31.0), give faster RCM of unhindered olefins compared to **6**–**7** (%*V*_{Bur} = 28.7 and 28.9), as well as slower RCM of hindered olefins. This hypothesis is supported by the behavior of the highly encumbered **HGII** (%*V*_{Bur} = 32.9), that outperforms catalysts **4**–**7** in the RCM of **8** and **10**, whereas it shows significantly lower efficiency in the RCM of **12**. On the other hand, no correlation between the electronic properties of different NHCs of **4**–**7** and the catalytic results can be easily established.

The catalytic performances of the newly synthesized complexes **4**–**7** were also compared in the RCM of (\pm)-linalool (**14**), a naturally occurring terpene alcohol, to form 1-methylcyclopent-2-en-1-ol and isobutylene, both representing valuable starting materials for the production of renewable fuels and polymer products.²² In line of principle, the RCM of this diolefin shows a significant steric deactivation because one of the double bonds is trisubstituted and the other one is flanked by a tetrasubstituted carbon. However, the reaction is facilitated by the activating effect of the allylic hydroxyl group which is able to interact with the catalytic center.²³ *Anti* complexes **5** and **7** turned out to be highly competent in this cyclization, giving full conversion in less than 2 min, while *syn* **6** behaves as **HGII** completing the reaction within 3 min (Fig. 9). The catalytic behavior of *syn* **4** was found

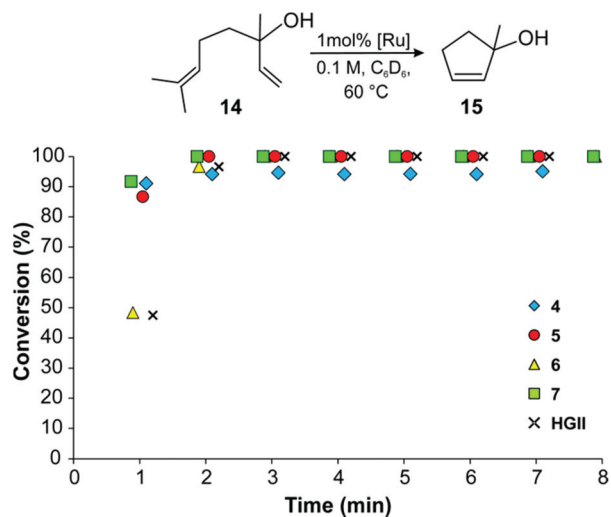


Fig. 9 RCM conversion of **14**.

to be somewhat different, since it reached a plateau at 94% conversion after the first minute of the reaction, suggesting a minor stability of this system with respect to all the other ones, very likely as a consequence of a deleterious interaction of the active species with the substrate or the product.

We next turned our attention to exploring the catalytic potential of **4–7** in CM reactions. First, the model CM of allyl

Table 2 CM of **16** and **17** promoted by catalysts **4–7**

Entry	Catalyst	38 yield ^a (%)	<i>E</i> : <i>Z</i> ^b
1	4	88	5.5
2	5	97	4.0
3	6	90	6.0
4	7	85	7.1
5	HGII	69	8.6

^a Isolated yield. ^b *E*:*Z* ratios were determined by ¹H NMR spectroscopy.

benzene (**16**) and *cis*-1,4-diacetoxy-2-butene (**17**) was investigated and the results are summarized in Table 2.

All of the catalysts furnished the desired cross-coupling product **18** in very high yields (85–97%), displaying better activities and lower *E/Z* ratios with respect to **HGII**. While changing the nature of the *N*-substituents did not affect the outcome of the reaction for *syn* catalysts **4** and **6** (entries 1 and 3), a different behavior was observed for *anti* catalysts **5** and **7** (entries 2 and 4), which exhibited different activities and *Z*-selectivities.

We then decided to probe the activity of **4–7** in cross-metathesis reactions involving biorenewable feedstocks as substrates to produce polyfunctional compounds. As an example, we selected the CM of eugenol acetate (**19**), a constituent of clove oil, with *cis*-1,4-dichloro-2-butene (**20**). This cross-metathesis led to the allylic chloride derivative **21** which can be subsequently transformed into a variety of useful chemicals.^{24,25} The reaction was carried out using 3 equivalents of **20** with respect to **19** (0.2 M) in the presence of 2.7 mol% of catalysts under refluxing CH₂Cl₂ for 12 h. All the results, including data for the CM performed using the benchmark catalyst **HGII**, are shown in Table 3.

In all cases, no undesired product arising from self-metathesis as well as from double-bond migration reactions was detected, as already observed in the analogous cross-metathesis of **19** with allyl-chloride.²⁴ Catalysts **4–7** were found to be more efficient than **HGII**, confirming that the presence of alkyl *N*-substituents is beneficial for this class of reactions. In more detail, **4** and **5** with *N*-neopentyl groups gave very low *E/Z* ratios, compared to **HGII** and previously reported catalytic systems.²⁴

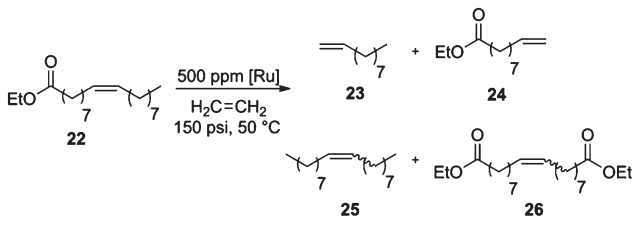
Ethenolysis of fatty acid esters represents another example of a cross-metathesis reaction that allows the selective conversion of renewable feedstock to useful products with extensive applications.²⁶ We therefore tested catalysts **4–7** in the ethenolysis of ethyl oleate (Table 4) comparing their performance to that of **HGII** at 50 °C using 500 ppm catalyst loading and 10 bar of ethylene.

As shown in Table 4 (entries 1–4), all the catalysts were scarcely active and selective, affording lower yields, selectivities and TONs with respect to **HGII**. These results not only point out that the introduction of alkyl instead of aryl groups as

Table 3 CM of **19** and **20** promoted by catalysts **4–7**

Entry	Catalyst	38 yield ^a (%)	<i>E</i> : <i>Z</i> ^b
1	4	88	2.8
2	5	70	3.2
3	6	84	5.4
4	7	77	5.4
5	HGII	52	7.4

^a Isolated yield. ^b *E*:*Z* ratios were determined by ¹H NMR spectroscopy.

Table 4 Ethenolysis of **22** promoted by catalysts 4–7


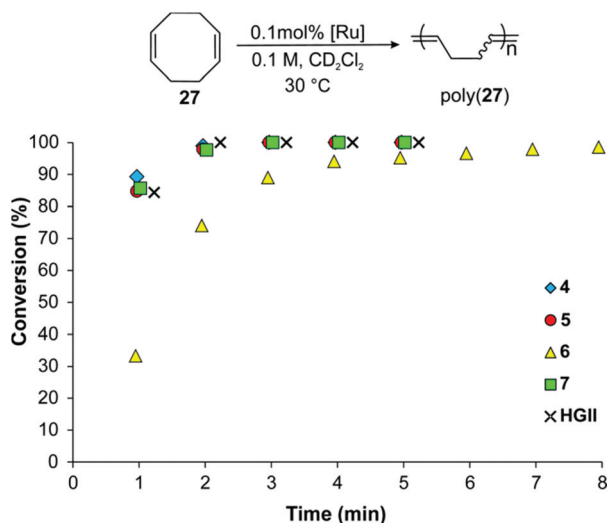
Entry	Catalyst ^a	Conversion z ^b (%)	Selectivity ^c (%)	Yield ^d (%)	TON ^e
1	4	50	35	18	350
2	5	28	37	10	207
3	6	25	32	8	160
4	7	49	20	10	196
5	HGII	71	43	30	600

^a The reactions were run neat using 5.4 mmol of ethyl oleate at 150 psi of ethylene. Dodecane (150 μ L) was used as an internal standard.

^b Determined by GC analysis. Conversion = $100 - (\text{final moles of } 22) \times 100 / [\text{initial moles of } 22]$. ^c Determined by GC analysis. Selectivity = $100 \times (\text{moles of ethenolysis products } 23 + 24) / [(\text{moles of } 23 + 24) + (2 \times \text{moles of } 25 + 26)]$. ^d Yield = conversion \times selectivity/100. ^e TON = yield \times (initial moles of **22**/moles of catalyst)/100.

N-substituents is detrimental for the performance of the catalyst in this kind of metathesis reaction, but they provide further evidence that such transformation is accomplished efficiently only in the presence of ruthenium catalysts bearing cyclic alkylaminocarbene (CAAC) ligands²⁷ or, to a lesser extent, with unsymmetrical NHCs.^{9c,28}

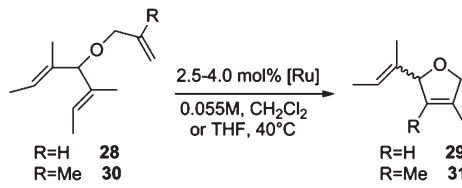
Then, the catalytic performances of 4–7 were evaluated in the ROMP of 1,5-cyclooctadiene (COD) carried out in C₆D₆, at 30 °C, in the presence of 0.1 mol% of catalyst. The reactions were monitored by ¹H NMR spectroscopy and the results are depicted in Fig. 10. For comparison, the kinetic profile of the ROMP promoted by the benchmark catalyst HGII is included.

**Fig. 10** ROMP conversion of **27**.

All complexes proved to be suitable catalysts for this reaction, especially **4**, **5** and **7** which showed no reactivity differences, converting COD quantitatively in less than 3 min and rivaling the performance of **HGII**. Catalyst **6** turned out as a less efficient system, completing the ROMP reaction within 9 min. The *E/Z* ratios of the double bonds in the polymer chains, determined by ¹H and ¹³C NMR spectroscopy, fall in a range between 1.4 and 1.8.

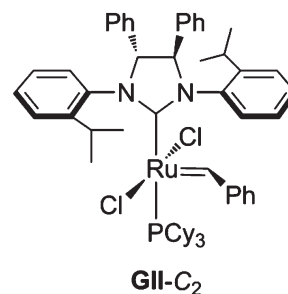
As a final investigation, we focused on the application of chiral *anti* catalysts **5** and **7** in the desymmetrization of achiral trienes **28** and **30** through asymmetric ring closing metathesis (ARCM), which represents a powerful means to obtain enantio-enriched carbo- and heterocycles.^{3,29} The results are summarized in Table 5.

The first chiral ruthenium-based metathesis catalysts having chiral C₂-symmetric NHC ligands were synthesized and evaluated in ARCM reactions by the Grubbs group (e.g. **GII-C₂**, Fig. 11).³⁰ In these systems, the chiral information is transferred from the backbone of the NHC ligand to the metal center through the *N*-bound aryl rings (gearing effect).³¹

Table 5 ARCM of **28** and **30** with catalysts **5** and **7**


Entry ^a	Substrate	Catalyst (mol%)	Additive	Yield ^b (%)	ee ^c (%)
1	28	5 (2.5)	None	>98	36 (<i>S</i>)
2	28	5 (4.0)	NaI	>98	15 (<i>R</i>)
3	28	7 (2.5)	None	>98	36 (<i>R</i>)
4	28	7 (4.0)	NaI	>98	13 (<i>R</i>)
5 ^d	28	GII-C₂ (2.5)	None	>98	35 (<i>S</i>)
6 ^d	28	GII-C₂ (4.0)	NaI	>98	90 (<i>S</i>)
7	30	5 (2.5)	None	>98	7 (<i>S</i>)
8	30	7 (2.5)	None	>98	33 (<i>S</i>)

^a Reactions without an additive were performed in CH₂Cl₂ at 40 °C for 2 h; reactions with NaI were carried out in THF at 40 °C for 2 h, after stirring **5** and **7** in solution of NaI for 1 h at RT. ^b Yields were based on NMR analysis. ^c Enantiomeric excesses determined by chiral GC. ^d Taken from ref. 30b.

**Fig. 11** Grubbs' catalyst bearing a C₂-symmetric NHC.

It should be highlighted that complexes **5** and **7** have the same NHC backbone substitution and configuration as the Grubbs chiral catalyst **GII-C₂** (Fig. 11), but they differ in the nature of the amino side groups (alkyl instead of aryl groups). Table 5 describes the results for the ARCM of model trienes **28** and **30** promoted by **5** and **7**. The available data for the ARCM of **28** performed with the catalyst **GII-C₂** are also reported. Both catalysts **5** and **7** provided dihydrofuran **29** in quantitative yield and 36% ee, albeit disclosing opposite enantioselectivity (entries 1 and 3, Table 5). In more detail, catalyst **5** with neopentyl *N*-substituents formed the same enantiomer as **GII-C₂**, while **7** with the cyclohexyl *N*-substituent catalyst gave the opposite one. In an attempt to improve the enantioselectivity of **5** and **7** by increasing the bulkiness of the halide ligands from chloride to iodide, as described for **GII-C₂** (entries 5 and 6),^{30b} lower enantiomeric excesses were obtained (entries 2 and 4). Moreover, in the ARCM reaction carried out in the presence of **5**, the inversion of the absolute configuration of **29** was observed.

These results confirm that the chiral substitution of the backbone is a key factor to achieve enantioinduction, albeit low. Even more, they suggest that a rigorously defined steric environment around the metal, deriving from the arrangement of the *N*-substituents (and in part from the bulkiness of the halide ligands), is crucial to define the stereochemical outcome of the reaction. Indeed, neopentyl and cyclohexyl *N*-substituents exhibit different degrees of adaptability and consequently they may contribute to delineate the shape of the reactive pocket in a very different way. This appears to be evident also in the more challenging ARCM of **30** to form a tetrasubstituted cycloolefin, where again different enantioselectivities between **5** and **7** were observed. It is worth noting that, to the best of our knowledge, this represents the first example of ARCM of **30** promoted by chiral ruthenium catalysts bearing a *C₂*-symmetric NHC ligand. In fact, only chiral complexes with the *C₁* symmetric NHC ligands have been tested so far, affording low to moderate enantioselectivities (up to 42% ee).^{9,32}

Experimental section

Synthesis of diamines A–C

Into a round bottom flask, under an inert atmosphere, the amine (1 eq.), anhydrous methylene chloride (*C* = 0.1 M) and activated molecular sieves were introduced. Then, the alkylating agent (pivalaldehyde, 5 eq. for **A**, 3 eq. for **B**; cyclohexanone, 10 eq. for **C**) was added. The reaction mixture was stirred under nitrogen for 48 hours at room temperature.

After filtration and removal of the solvent under reduced pressure, the crude reaction product was diluted with dry methanol (*C* = 0.1 M) and treated with NaBH₄ (equimolar with respect to the alkylating agent, added in three portions). The mixture was stirred at room temperature for 3.5 hours under nitrogen. The crude product was extracted with water and methylene chloride. The organic layer was dried over sodium

sulphate and then the solvent was removed under vacuum. The product, obtained as a yellow oil, was purified using column chromatography on silica gel (hexane/ethyl acetate 9/1) to afford a white solid.

A (MW = 352.6 g mol⁻¹) yield 94%. ¹H NMR (CD₂Cl₂, 300 MHz): δ 7.24–7.19 (o m, 10H, Ar–H); 3.67 (s, 2H, N–CH–CH–N); 2.12 (d, ³*J* = 0.7 Hz, 2H, –CH₂–C(CH₃)₃); 2.07 (d, ³*J* = 1.6 Hz, 2H, CH₂–C(CH₃)₃); 0.77 (s, 18H, CH₂–C(CH₃)₃). ¹³C{H} NMR (CD₂Cl₂, 75 MHz): δ 142.1; 128.5; 127.9; 127.0; 69.1; 59.9; 31.4; 30.8; 27.5. ESI + MS: *m/z* = 353.1 (MH⁺). Anal. calcd for C₂₄H₃₆N₂ (352.56): C, 81.76, H, 10.29, N, 7.95. Found: C, 81.82, H, 10.38, N, 7.89.

B (MW = 352.6 g mol⁻¹) yield 76%. ¹H NMR (CDCl₃, 300 MHz): δ 7.28–7.26 (o m, 3H, Ar–H); 7.16–7.13 (o m, 3H, Ar–H); 3.68 (s, 2H, N–CH–CH–N); 2.37–2.26 (q, ³*J* = 11.1 Hz, ³*J* = 8.2 Hz, 4H, CH₂–C(CH₃)₃); 1.07 (s, 18H, CH₂–C(CH₃)₃). ¹³C{H} NMR (CD₂Cl₂, 75 MHz): δ 142.3; 128.0; 127.8; 126.7; 70.7; 60.2; 31.8; 27.9. ESI + MS: *m/z* = 353.3 (MH⁺). [α]_D²⁰ = –6.9° (*c* = 0.5 in CH₂Cl₂). Anal. calcd for C₂₄H₃₆N₂ (352.56): C, 81.76, H, 10.29, N, 7.95. Found: C, 81.84, H, 10.41, N, 7.88.

C (MW = 376.6 g mol⁻¹) yield 77%. ¹H NMR (CDCl₃, 300 MHz): δ 7.28–7.20 (o m, 10H, Ar–H); 3.90 (s, 2H, N–CH–CH–N); 2.12–2.07 (br t, 2H, N–CH(Cy)); 1.75–1.73 (o m, 2H, Cy–H); 1.55–1.44 (o m, 10H, Cy–H); 1.06–0.91 (o m, 6H, Cy–H); 0.77–0.75 (o m, 2H, Cy–H). ¹³C{H} NMR (CDCl₃, 75 MHz): δ 142.0; 128.5; 128.2; 127.3; 65.1; 53.1; 34.8; 32.4; 26.2; 25.1; 24.7. ESI + MS: *m/z* = 377.4 (MH⁺). Anal. calcd for C₂₆H₃₆N₂ (376.58): C, 82.93, H, 9.64, N, 7.44. Found: C, 83.01, H, 9.68, N, 7.58.

Synthesis of D

For the synthesis of **D**, a two-step procedure was used. In the first step, the monoalkylated diamine was prepared as previously reported.^{9a} A round bottom flask was charged with the diamine (1 eq.), cyclohexanone (3 eq.) and anhydrous methylene chloride (*C* = 0.1 M). The reaction mixture was stirred for 12 hours at room temperature over activated molecular sieves. After filtration, the solvent was removed under reduced pressure and anhydrous methanol was added (*C* = 0.1 M). The resulting solution was stirred at room temperature for 30 minutes and then diluted with methanol (*C* = 0.05 M as final concentration). NaBH₄ (4 eq.) was added portionwise under a nitrogen atmosphere and the reaction mixture was stirred for 3.5 h. After extraction from dichloromethane–water, the organic layer was dried over anhydrous sodium sulphate and then the solvent was removed under vacuum to afford the monoalkylated diamine as a colourless oil (92%). In the second step, the monoalkylated product was dissolved in CHCl₃ (*C* = 0.1 M) and reacted with cyclohexanone (10 eq.) in the presence of two drops of HCOOH at 50 °C for 48 h. To the resulting imine, after filtration and removal of the solvent under reduced pressure, dry methanol (*C* = 0.1 M) and NaBH₄ (equimolar with respect to cyclohexanone, added in three portions) were added. The mixture was stirred at room temperature for 3.5 hours under nitrogen. The crude product was extracted with water and methylene chloride. The organic layer

was dried over sodium sulphate and then the solvent was removed under vacuum. The product was obtained as a white powder after purification by column chromatography (hexane/ethyl acetate 9/1).

D (MW = 376.6 g mol⁻¹) yield 64%. ¹H NMR (CDCl₃, 400 MHz): δ 7.15–7.08 (o m, 6H, Ar-H); 7.03–7.01 (o m, 4H, Ar-H); 3.73 (s, 2H, N-CH-CH-N); 2.19 (br t, 2H, N-CH(Cy)); 1.90–1.85 (o m, 4H, Cy-H); 1.63–1.47 (o m, 9H, Cy-H); 1.11–1.00 (o m, 7H, Cy-H). ¹³C{H} NMR (CDCl₃, 100 MHz): δ 142.7; 128.0; 127.8; 126.6; 66.4; 53.9; 35.1; 32.7; 26.3; 25.5; 24.8. ESI + MS: *m/z* = 378.2 (MH⁺).

[α]_D²⁰ = -26.8° (*c* = 0.5 in CH₂Cl₂). Anal. calcd for C₂₆H₃₆N₂ (376.58): C, 82.93, H, 9.64, N, 7.44. Found: C, 82.98, H, 9.70, N, 7.54.

Synthesis of imidazolinium salts E-H

Into a flask containing the diamine (1 eq.), triethyl orthoformate (8 eq.) and NH₄BF₄ (1.2 eq.) were introduced. The reaction mixture was stirred at 135 °C for 4 hours. The crude product obtained as a brownish oil was washed with diethyl ether and purified on column chromatography (hexane/ethyl acetate 1/1). Imidazolinium salts were obtained as white solids.

E (MW = 450.4 g mol⁻¹) yield 87%. ¹H NMR (CDCl₃, 400 MHz): δ 8.82 (s, 1H, N-CH-N); 7.15 (br s, 5H, Ar-H); 6.91 (br s, 4H, Ar-H); 5.70 (s, 2H, N-CH-CH-N); 3.79 (d, ³*J* = 14.3 Hz, 2H, N-CH₂-C(CH₃)₃); 2.91 (d, ³*J* = 14.3 Hz, 2H, -CH₂-C(CH₃)₃); 1.00 (s, 18H, CH₂-C(CH₃)₃). ¹³C{H} NMR (CDCl₃, 100 MHz): δ 162.6; 131.4; 130.5; 130.1; 129.7; 73.0; 58.7; 34.4; 28.9. ESI + MS: *m/z* = 363.1 (MH⁺ - BF₄⁻). Anal. calcd for C₂₅H₃₅BF₄N₂ (450.36): C, 66.67, H, 7.83, N, 6.22. Found: C, 66.75, H, 7.90, N, 6.31.

F (MW = 450.4 g mol⁻¹) yield 87%. ¹H NMR (CDCl₃, 250 MHz): δ 8.98 (s, 1H, N-CH-N); 7.54–7.52 (o m, 6H, Ar-H); 7.24–7.23 (o m, 4H, Ar-H); 5.05 (s, 2H, N-CH-CH-N); 3.67 (d, ³*J* = 14.5 Hz, 2H, N-CH₂-C(CH₃)₃); 2.92 (d, ³*J* = 14.5 Hz, 2H, N-CH₂-C(CH₃)₃); 0.97 (s, 18H, CH₂-C(CH₃)₃). ¹³C{H} NMR (CDCl₃, 62.5 MHz): δ 160.9; 135.4; 130.5; 126.6; 75.6; 57.4; 33.2; 27.9. ESI + MS: *m/z* = 363.2 (MH⁺ - BF₄⁻). [α]_D²⁰ = 417.9 (*c* = 0.5 in CH₂Cl₂). Anal. calcd for C₂₅H₃₅BF₄N₂ (450.36): C, 66.67, H, 7.83, N, 6.22. Found: C, 66.74, H, 7.92, N, 6.28.

G (MW = 474.4 g mol⁻¹) yield 91%. ¹H NMR (CDCl₃, 300 MHz): δ 9.51 (s, 1H, N-CH-N); 7.08–7.05 (o m, 6H, Ar-H); 6.89–6.86 (o m, 4H, Ar-H); 5.81 (s, 2H, N-CH-CH-N); 3.22 (br t, 2H, N-CH(Cy)); 2.18–2.11 (o m, 3H, Cy-H); 2.05–1.98 (o m, 4H, Cy-H); 1.86–1.83 (o m, 2H, Cy-H); 1.70–1.66 (o m, 2H, Cy-H); 1.52–1.41 (o m, 4H, Cy-H); 1.28–1.01 (o m, 5H, Cy-H). ¹³C{H} NMR (CDCl₃, 75 MHz): δ 157.0; 131.6; 128.9; 128.6; 128.2; 68.4; 57.4; 32.1; 31.3; 25.4; 25.1; 24.8. ESI + MS: *m/z* = 389.1 (MH⁺ - BF₄⁻). Anal. calcd for C₂₇H₃₅BF₄N₂ (474.38): C, 68.36, H, 7.44, N, 5.91. Found: C, 68.44, H, 7.41, N, 6.08.

H (MW = 474.4 g mol⁻¹) yield 87%. ¹H NMR (CDCl₃, 400 MHz): δ 8.78 (s, 1H, N-CH-N); 7.50–7.47 (o m, 6H, Ar-H); 7.23–7.20 (o m, 4H, Ar-H); 4.86 (s, 2H, N-CH-CH-N); 3.39 (tt, ³*J* = 3.6 Hz, ³*J* = 3.6 Hz, 2H, N-CH(Cy)); 2.04–2.01 (o m, 2H, Cy-H); 1.90–1.83 (o m, 5H, Cy-H); 1.78–1.69 (o m, 5H, Cy-H);

1.29–1.11 (o m, 8H, Cy-H). ¹³C{H} NMR (CDCl₃, 100 MHz): δ 155.0; 136.8; 130.1; 126.6; 72.3; 57.8; 32.1; 31.1; 25.2; 25.0; 24.7. ESI + MS: *m/z* = 389.1 (MH⁺ - BF₄⁻).

[α]_D²⁰ = 152.5° (*c* = 0.5 in CH₂Cl₂). Anal. calcd for C₂₇H₃₅BF₄N₂ (474.38): C, 68.36, H, 7.44, N, 5.91. Found: C, 68.48, H, 7.47, N, 6.02.

General procedure for the synthesis of ruthenium complexes

4-7

Under an inert atmosphere, a Schlenk tube was charged with the tetrafluoroborate salt (1.2 eq.), the base (CF₃(CH₃)₂COK for **5** and CH₃CH₂(CH₃)₂COK for **4**, **6** and **7**, 1.2 eq.) and dry toluene (*C* = 0.026 M for **4**, **6** and **7**, *C* = 0.1 M for **5**). After a few minutes, the first generation Hoveyda-Grubbs catalyst (0.5 eq.) was added. The reaction mixture was heated to 65 °C for two hours (**5**) or for 50 minutes (**4**, **6** and **7**) and was then purified with column chromatography on silica gel (hexane/diethyl ether from 9/1 to 2/1) to afford the ruthenium catalysts as green solids.

4 (MW = 682.7 g mol⁻¹) yield 40%. ¹H NMR (C₆D₆, 400 MHz): δ 18.48 (s, 1H, Ru=CH-*o*OiPrC₆H₄); 7.64 (br s, 3H, Ar-H); 7.45 (d, ³*J* = 7.6 Hz, 1H, Ar-H); 7.26 (t, ³*J* = 8.1 Hz, 1H, Ar-H); 7.10–6.73 (o m, 7H, Ar-H); 6.55 (d, ³*J* = 8.1 Hz, 2H, Ar-H); 5.55 (br s, 3H, N-CH-CH-N and N-CH(H)-C(CH₃)₃); 4.88–4.70 (o m, 2H, O-CH(CH₃)₂ and N-CH(H)-C(CH₃)₃); 3.51 (d, ³*J* = 14.0 Hz, 2H, N-CH₂-C(CH₃)₃); 1.79 (br s, 6H, O-CH(CH₃)₂); 1.37–0.98 (o m, 18H, CH₂-C(CH₃)₃). ¹³C{H} NMR (C₆D₆, 75 MHz): δ 286.2 (Ru=CH-*o*OiPrC₆H₄); 210.9; 154.2; 144.9; 122.6; 122.1; 113.7; 75.3; 29.4; 22.1. Anal. calcd for C₃₅H₄₆Cl₂N₂ORu (682.73): C, 61.57, H, 6.79, N, 4.10. Found: C, 61.68, H, 6.84, N, 4.15. ESI-FT-ICR (**4**-Cl): *m/z* = calc. 647.2342, found 647.23338.

5 (MW = 682.7 g mol⁻¹) yield 62%. ¹H NMR (C₆D₆, 600 MHz): δ 18.71 (s, 1H, Ru=CH-*o*OiPrC₆H₄); 7.63 (br s, 4H, Ar-H); 7.53 (d, ³*J* = 7.6 Hz, 1H, Ar-H); 7.30–7.24 (o m, 5H, Ar-H); 7.08 (t, ³*J* = 7.8 Hz, 2H, Ar-H); 6.78 (t, ³*J* = 7.4 Hz, 1H, Ar-H); 6.57 (d, ³*J* = 8.3 Hz, 1H, Ar-H); 5.66 (br d, 1H, N-CH(H)-C(CH₃)₃); 4.91 (br s, 3H, N-CH-CH-N and N-CH(H)-C(CH₃)₃); 4.73 (m, 1H, O-CH(CH₃)₂); 3.66 (br d, 1H, N-CH(H)-C(CH₃)₃); 3.00 (br d, 1H, N-CH(H)-C(CH₃)₃); 1.77 (dd, ³*J* = 6.2 Hz, 6H, O-CH(CH₃)₂); 1.11 (br s, 9H, CH₂-C(CH₃)₃); 0.88 (br s, 9H, CH₂-C(CH₃)₃). ¹³C{H} NMR (C₆D₆, 125 MHz): δ 286.8 (Ru=CH-*o*OiPrC₆H₄); 209.8; 153.9; 145.4; 139.6; 130.0; 129.9; 129.2; 129.0; 128.7; 127.7; 127.2; 123.2; 123.0; 114.1; 76.6; 75.6; 74.2; 61.5; 58.1; 34.0; 33.5; 29.5; 29.4; 22.9; 22.8; 22.7; 22.6. Anal. calcd for C₃₅H₄₆Cl₂N₂ORu (682.73): C, 61.57, H, 6.79, N, 4.10. Found: C, 61.65, H, 6.86, N, 4.14. ESI-FT-ICR (**5**-Cl): *m/z* = calc. 647.2342, found 647.23335.

6 (MW = 706.8 g mol⁻¹) yield 60%. ¹H NMR (C₆D₆, 400 MHz): δ 18.25 (s, 1H, Ru=CH-*o*OiPrC₆H₄); 7.72–7.35 (o m, 3H, Ar-H); 7.28 (t, ³*J* = 7.5 Hz, 1H, Ar-H); 6.93–6.79 (o m, 8H, Ar-H); 6.60 (d, ³*J* = 8.3 Hz, 1H, Ar-H); 6.54 (br s, 1H, Ar-H); 5.27 (br s, 1H, N-CH(Cy)); 5.15 (s, 2H, N-CH-CH-N); 5.04 (br s, 1H, N-CH(Cy)); 4.76 (m, 1H, O-CH(CH₃)₂); 2.88 (br s, 1H, Cy-H); 2.31 (br s, 1H, Cy-H); 2.03–1.66 (o m, 11H, O-CH(CH₃)₂ and Cy-H); 1.54–0.68 (o m, 13H, Cy-H). ¹³C{H} NMR (C₆D₆,

100 MHz): δ 284.2 (Ru=CH-*o*OiPrC₆H₄); 217.8; 154.2; 144.7; 137.5; 129.8; 129.2; 122.7; 122.1; 113.6; 75.1; 68.0; 62.9; 61.7; 33.9; 26.4; 25.6; 22.2. Anal. calcd for C₃₇H₄₆Cl₂N₂ORu (706.75): C, 62.88, H, 6.56, N, 3.96. Found: C, 62.94, H, 6.79, N, 4.07. ESI-FT-ICR (6-Cl): m/z = calc. 671.2342, found 671.2332.

7 (MW = 706.8 g mol⁻¹) yield 53%. ¹H NMR (C₆D₆, 400 MHz): δ 18.43 (s, 1H, Ru=CH-*o*OiPrC₆H₄); 7.53 (d, ³J = 6.5 Hz, 4H, Ar-H); 7.32–7.23 (o m, 6H, Ar-H); 7.10 (t, ³J = 7.4 Hz, 2H, Ar-H); 6.82 (t, ³J = 7.5 Hz, 1H, Ar-H); 6.59 (d, ³J = 8.4 Hz, 1H, Ar-H); 5.57 (br s, 1H, N-CH(Cy)); 5.05 (br s, 1H, N-CH(Cy)); 4.75 (m, 1H, O-CH(CH₃)₂); 4.48 (s, 2H, N-CH-CH-N); 2.57 (br s, 2H, Cy-H); 2.04 (br s, 2H, Cy-H); 1.80 (dd, ³J = 6.1 Hz, 6H, O-CH(CH₃)₂); 1.67–0.63 (o m, 18H, Cy-H). ¹³C{¹H} NMR (C₆D₆, 100 MHz): δ 286.2 (Ru=CH-*o*OiPrC₆H₄); 211.0; 154.3; 145.0; 129.5; 129.3; 122.7; 122.2; 113.8; 29.5; 22.2; 21.7. Anal. calcd for C₃₇H₄₆Cl₂N₂ORu (706.75): C, 62.88, H, 6.56, N, 3.96. Found: C, 62.96, H, 6.77, N, 4.05. ESI-FT-ICR (7-Cl): m/z = calc. 671.2342, found 671.2349.

Conclusions

In conclusion, we have prepared four new stable Hoveyda-Grubbs second generation catalysts featuring symmetrically *N*-alkyl substituted NHCs with neopentyl or cyclohexyl groups at the nitrogens and phenyl substituents on the backbone in a *syn* or an *anti* stereochemical relationship (4–7). Synthetic access to these complexes and their isolation were strongly facilitated by the introduction of suitable backbone substitution, which allowed obtaining, for the first time, olefin metathesis ruthenium catalysts bearing saturated NHCs with primary *N*-alkyl groups (4, 5). This finding opens the way to the development of new ligands with significantly different encumbrance around the metal. A detailed description of 4–7 was provided in terms of steric and electronic differences of their NHC ligands. According to %V_{Bur} analysis, *N,N'*-dineopentyl substituted NHCs of 4 and 5 were found to offer a more pronounced and asymmetrically distributed steric hindrance around the metal with respect to *N,N'*-dicyclohexyl NHCs of 6 and 7, which, on the other hand, exhibited better electron donating properties, as evidenced by electrochemical studies. As for the NHC backbone configuration, no remarkable effect was observed. A comparison of the catalytic properties of 4–7 with those of the reference catalyst (HGII) revealed that they give better performances in most of the explored transformations. In particular, they were found to be more competent for the RCM reactions leading to the formation of a tetrasubstituted double bond and for CM reactions, for which improved *Z*-selectivities were also observed, especially in the CM of eugenol acetate with *cis*-1,4-dichlorobutene. While RCM activities appear to be mainly related to the bulkiness of the *N*-groups, CM activities and selectivities seem to be dependent also on the relative orientation of substituents on the NHC backbone, although to a lesser extent and following a trend more difficult to interpret. Catalysts 5 and 7 bearing chiral C₂ symmetric NHCs were tested in the ARCM of model achiral

trienes. Even if modest enantioselectivities were observed, this study confirms the relevance of the backbone configuration to give enantioinduction and suggests also that the different nature of *N*-alkyl groups may influence the stereochemical outcome of the reaction. We are currently exploring alternative pathways for the synthesis of new *N,N'*-dialkyl NHC architectures, including the unsymmetrical ones, to provide new opportunities in catalyst design and metathesis applications.

Conflicts of interest

There are no conflicts to declare.

Acknowledgements

The authors thank Dr Patrizia Iannece and Dr Patrizia Oliva for technical assistance. Mr Raffaele Contino, who performed some experiments, is kindly acknowledged. This work was financed by the Ministero dell'Università e della Ricerca Scientifica e Tecnologica. Financial support from POR CAMPANIA FESR 2007/2013 O.O. 2.1. – CUP B46D14002660009 “Il potenziamento e la riqualificazione del sistema delle infrastrutture nel settore dell'istruzione, della formazione e della ricerca” is gratefully acknowledged.

References

- (a) H.-W. Wanzlick and H.-J. Schönherr, *Angew. Chem., Int. Ed. Engl.*, 1968, 7, 141; (b) K. Öfele, *J. Organomet. Chem.*, 1968, 12, P42.
- (a) E. Peris, *Chem. Rev.*, DOI: 10.1021/acs.chemrev.6b00695; (b) D. Jansenn-Müller and F. Glorius, *Chem. Soc. Rev.*, 2017, 46, 4845; (c) D. M. Flanigan, F. Romanov-Michailidis, N. A. White and T. Rovis, *Chem. Rev.*, 2015, 115, 9307; (d) *N-Heterocyclic Carbenes: Effective Tools for Organometallic Synthesis*, ed. S. P. Nolan, Wiley-VCH, 2014; (e) M. N. Hopkinson, C. Richter, M. Schedler and F. Glorius, *Nature*, 2014, 510, 485; (f) C. S. J. Cazin, *N-Heterocyclic Carbenes in Transition Metal Catalysis and Organocatalysis*, Springer, 2011; (g) D. Enders, O. Niemeier and A. Henseler, *Chem. Rev.*, 2007, 107, 5606; (h) *N-Heterocyclic Carbenes in Transition Metal catalysis*, ed. F. Glorius, Springer-Verlag, Berlin, Germany, 2007; (i) A. Correa, S. P. Nolan and L. Cavallo, *Top. Curr. Chem.*, 2011, 302, 131; (j) *N-Heterocyclic Carbenes*, ed. S. Diez-González, Royal Society of Chemistry, 2011; (k) D. Enders and A. Grossmann, *Angew. Chem., Int. Ed.*, 2012, 51, 314; (l) L. Benhamou, E. Chardon, G. Lavigne, S. Bellemin-Laponnaz and V. César, *Chem. Rev.*, 2011, 111, 2705; A. T. Biju, N. Kuhl and F. Glorius, *Acc. Chem. Res.*, 2011, 44, 1182; (m) M. Fevre, J. Pinaud, Y. Gnanou, J. Vignolle and D. Taton, *Chem. Soc. Rev.*, 2013, 42, 2142.
- (a) R. H. Grubbs, A. G. Wenzel, D. J. O'Leary and E. Khosravi, *Handbook of Metathesis*, Wiley-VCH,

- Weinheim, Germany, 2nd edn, 2015; (b) *Olefin Metathesis Theory and Practice*, ed. K. Grela, J. Wiley & Sons, Hoboken, NJ, 2014.
- 4 (a) G. C. Vougioukalakis and R. H. Grubbs, *Chem. Rev.*, 2010, **110**, 1746; (b) C. Samojlowicz, M. Bieniek and K. Grela, *Chem. Rev.*, 2009, **109**, 3708.
 - 5 Selected examples: (a) T. J. Seiders, D. W. Ward and R. H. Grubbs, *Org. Lett.*, 2001, **3**, 3225; (b) T. Ritter, M. W. Day and R. H. Grubbs, *J. Am. Chem. Soc.*, 2006, **128**, 11768; (c) I. C. Stewart, T. Ung, A. A. Pletnev, J. M. Berlin, R. H. Grubbs and Y. Schrodi, *Org. Lett.*, 2007, **9**, 1589; (d) J. M. Berlin, K. Campbell, T. Ritter, T. W. Funk, A. Chlenov and R. H. Grubbs, *Org. Lett.*, 2007, **9**, 1339; (e) C. K. Chung and R. H. Grubbs, *Org. Lett.*, 2008, **10**, 2693; (f) K. M. Kuhn, J.-B. Bourg, C. K. Chung, S. C. Virgil and R. H. Grubbs, *J. Am. Chem. Soc.*, 2009, **131**, 5313; (g) M. Gatti, L. Vieille-Petit, X. Luan, R. Mariz, E. Drinkel, A. Linden and R. Dorta, *J. Am. Chem. Soc.*, 2009, **131**, 9498; (h) L. Vieille-Petit, X. Luan, M. Gatti, S. Blumentritt, A. Linden, H. Clavier, S. P. Nolan and R. Dorta, *Chem. Commun.*, 2009, 3783; (i) T. Savoie, B. Stenne and S. K. Collins, *Adv. Synth. Catal.*, 2009, **351**, 1826; (j) A. Perfetto, V. Bertolasi, C. Costabile, V. Paradiso, T. Caruso, P. Longo, and F. Grisi, *RSC Adv.*, 2016, **6**, 95793.
 - 6 (a) N. Ledoux, B. Allaert, S. Pattyn, H. V. Mierde, C. Vercaemst and F. Verpoort, *Chem. – Eur. J.*, 2006, **12**, 4654; (b) N. Ledoux, A. Linden, B. Allaert, H. V. Mierde and F. Verpoort, *Adv. Synth. Catal.*, 2007, **349**, 1692; (c) F. Grisi, C. Costabile, E. Gallo, A. Mariconda, C. Tedesco and P. Longo, *Organometallics*, 2008, **27**, 4649.
 - 7 (a) A. Poater, F. Ragone, S. Giudice, C. Costabile, R. Dorta, S. P. Nolan and L. Cavallo, *Organometallics*, 2008, **27**, 2681; (b) M. B. Dinger, P. Nieczypor and J. C. Mol, *Organometallics*, 2003, **22**, 5291.
 - 8 (a) F. Grisi, A. Mariconda, C. Costabile, V. Bertolasi and P. Longo, *Organometallics*, 2009, **28**, 4988; (b) C. Costabile, A. Mariconda, L. Cavallo, P. Longo, V. Bertolasi, F. Ragone and F. Grisi, *Chem. – Eur. J.*, 2011, **17**, 8618; (c) A. Perfetto, C. Costabile, P. Longo, V. Bertolasi and F. Grisi, *Chem. – Eur. J.*, 2013, **19**, 10492; (d) A. Perfetto, C. Costabile, P. Longo and F. Grisi, *Organometallics*, 2014, **33**, 2747.
 - 9 (a) V. Paradiso, V. Bertolasi and F. Grisi, *Organometallics*, 2014, **33**, 5932; (b) V. Paradiso, V. Bertolasi, C. Costabile and F. Grisi, *Dalton Trans.*, 2016, **45**, 561; (c) V. Paradiso, V. Bertolasi, C. Costabile, F. Grisi, T. Caruso, M. Dąbrowski, K. Grela and F. Grisi, *Organometallics*, 2017, **36**, 3692.
 - 10 V. Paradiso, C. Costabile and F. Grisi, *Molecules*, 2016, **21**, 117.
 - 11 (a) L. H. Peeck and H. Plenio, *Organometallics*, 2010, **29**, 2761; (b) S. Wolf and H. Plenio, *Green Chem.*, 2011, **13**, 2008; (c) C. S. Higman, S. A. Ruff, R. McDonald and D. E. Fogg, *J. Organomet. Chem.*, 2017, **847**, 162.
 - 12 The synthesis of 4–7 was accomplished by using both potassium hexafluoro-*t*-butoxide or potassium *t*-amylate for the deprotonation *in situ* of the related NHC salts. In this work, we reported the most successful synthetic route identified for each catalyst.
 - 13 M. N. Burnett and C. K. Johnson, *ORTEP III*, Oak Ridge National Laboratory, Oak Ridge, TN, 1996; Report ORNL-6895.
 - 14 L. Falivene, R. Credendino, A. Poater, A. Petta, L. Serra, R. Oliva, V. Scarano and L. Cavallo, *Organometallics*, 2016, **35**, 2286 % V_{Bur} is a parameter to quantify the steric hindrance of NHC ligands defined as the fraction of the total volume of a sphere centered on the metal occupied by a given ligand: (a) R. Dorta, E. D. Stevens, N. M. Scott, C. Costabile, L. Cavallo, C. D. Hoff and S. P. Nolan, *J. Am. Chem. Soc.*, 2005, **127**, 2485; (b) L. Cavallo, A. Correa, C. Costabile and H. Jacobsen, *J. Organomet. Chem.*, 2005, **690**, 5407.
 - 15 M. M. Wu, A. M. Gill, L. Yunpeng, L. Falivene, L. Yongxin, R. Ganguly, L. Cavallo and F. Garcia, *Dalton Trans.*, 2015, **44**, 15166.
 - 16 M. Süßner and H. Plenio, *Chem. Commun.*, 2005, **43**, 5417.
 - 17 (a) K. Verlinden, H. Buhl, W. Frank and C. Ganter, *Eur. J. Inorg. Chem.*, 2015, 2416; (b) M. Ruamps, N. Lugan and V. César, *Organometallics*, 2017, **36**, 1049.
 - 18 H. A. Bent, *Chem. Rev.*, 1961, **61**, 275.
 - 19 (a) H. Jacobsen, A. Correa, C. Costabile and L. Cavallo, *J. Organomet. Chem.*, 2006, **691**, 4350; (b) H. Jacobsen, A. Correa, A. Poater, C. Costabile and L. Cavallo, *Coord. Chem. Rev.*, 2009, **253**, 687; (c) J. A. M. Lummiss, C. S. Higman, D. L. Fyson, R. McDonald and D. E. Fogg, *Chem. Sci.*, 2015, **6**, 6739.
 - 20 N. Mukherjee, S. Planer and K. Grela, *Org. Chem. Front.*, 2018, **82**, 494.
 - 21 T. Ritter, A. Hejl, A. G. Wenzel, T. W. Funk and R. H. Grubbs, *Organometallics*, 2006, **25**, 5740.
 - 22 Selected examples: (a) H. A. Meylemans, R. L. Quintana, B. R. Goldsmith and B. G. Harvey, *ChemSusChem*, 2011, **4**, 465; (b) R. Alcántara, E. Alcántara, L. Canoira, M. J. Franco, M. Herera and A. Navarro, *React. Funct. Polym.*, 2000, **45**, 19; (c) J. W. Yoon, S. H. Jhung, T.-J. Kim, H.-D. Lee, N. H. Jang and J.-S. Chang, *Bull. Korean Chem. Soc.*, 2007, **28**, 2075; (d) Y. Li, Y. Wu, L. Liang, Y. Li and G. Wu, *Chin. J. Polym. Sci.*, 2010, **28**, 55; (e) V. Vasilenko, A. N. Frolov and S. V. Kostjuk, *Macromolecules*, 2010, **43**, 5503; (f) J. S. Chickos, A. E. Wentz and D. Hillesheim-Cox, *Ind. Eng. Chem. Res.*, 2003, **42**, 2874–2877.
 - 23 T. R. Hoye and H. Zhao, *Org. Lett.*, 1999, **1**, 1123.
 - 24 H. Bilel, N. Hamdi, F. Zagrouba, C. Fischmeister and C. Bruneau, *Catal. Sci. Technol.*, 2014, **4**, 2064.
 - 25 Some examples of functionalized allyl chlorides as value added chemical intermediates are reported in: (a) M. Bandini, P. G. Cozzi, S. Licciulli and A. Umani-Ronchi, *Synthesis*, 2004, **3**, 409; (b) T. Jacobs, A. Rybak and M. A. R. Meier, *Appl. Catal., A*, 2009, **353**, 32.
 - 26 (a) J. C. Mol, *Green Chem.*, 2002, **4**, 5; (b) S. Chikkali and S. Mecking, *Angew. Chem., Int. Ed.*, 2012, **51**, 5802; (c) L. Montero de Espinosa and M. A. R. Meier, *Top. Organomet. Chem.*, 2012, **39**, 1; (d) J. Bidange, C. Fischmeister and C. Bruneau, *Chem. – Eur. J.*, 2016, **22**,

- 12226; (e) J. Spekrijse, J. P. M. Sanders, J. H. Bitter and E. L. Scott, *ChemSusChem*, 2017, **10**, 470.
- 27 (a) D. R. Anderson, V. Lavallo, D. J. O'Leary, G. Bertrand and R. H. Grubbs, *Angew. Chem., Int. Ed.*, 2007, **46**, 7262; (b) D. R. Anderson, T. Ung, G. Mkrtumyan, G. Bertrand and R. H. Grubbs, *Organometallics*, 2008, **27**, 563; (c) Y. Schrodi, T. Ung, A. Vargas, G. Mkrtumyan, W.-C. Lee, T. M. Champagne, R. L. Pederson and S. H. Hong, *Clean: Soil, Air, Water*, 2008, **36**, 669; (d) J. Zhang, S. Song, X. Wang, J. Jiao and M. Shi, *Chem. Commun.*, 2013, **49**, 9491; (e) V. M. Marx, A. H. Sullivan, M. Melaimi, S. C. Virgil, B. K. Keitz, D. S. Weinberger, G. Bertrand and R. H. Grubbs, *Angew. Chem., Int. Ed.*, 2015, **54**, 1919; (f) R. Gawin, A. Kozakiewicz, P. A. Guńka, P. Dąbrowski and K. Skowerski, *Angew. Chem., Int. Ed.*, 2017, **56**, 981.
- 28 R. M. Thomas, B. K. Keitz, T. M. Champagne and R. H. Grubbs, *J. Am. Chem. Soc.*, 2011, **133**, 7490.
- 29 (a) T. Patrick Montgomery, A. M. Johns and R. H. Grubbs, *Catalysts*, 2017, **7**, 87; (b) S. Kress and S. Blechert, *Chem. Soc. Rev.*, 2012, **41**, 4389; (c) A. H. Hoveyda and R. R. Schrock, *Chem. – Eur. J.*, 2001, **7**, 945.
- 30 (a) T. J. Seiders, D. W. Ward and R. H. Grubbs, *Org. Lett.*, 2001, **3**, 3225; (b) T. W. Funk, J. M. Berlin and R. H. Grubbs, *J. Am. Chem. Soc.*, 2006, **128**, 1840.
- 31 C. Costabile and L. Cavallo, *J. Am. Chem. Soc.*, 2004, **126**, 9592.
- 32 (a) B. Stenne, J. Timperio, J. Savoie, T. Dudding and S. K. Collins, *Org. Lett.*, 2010, **12**, 2032; (b) V. Paradiso, S. Menta, M. Pierini, G. Della Sala, A. Ciogli and F. Grisi, *Catalysts*, 2016, **6**, 177.